Original Article

Canine vertebral screw and rod fixation system in dogs

Murshidah Mohd Asri[2] Lau Seng Fong[1] Rozanaliza Radzi[1] Mazlina Mazlan[3]

Pakthorn Lewchalermwong[4] Björn Meij[5] Intan Nur Fatiha Shafie[1*]

Abstract

Bone plates and screws are often recommended to fix vertebral fracture and luxation in dogs although several complications had been reported. The canine vertebral screw and rod fixation (CVSRF) system, a device tailored for the canine spine, is a modified system from the human pedicle screw. This study aimed to determine the optimal corridor implantation of CVSRF and to investigate the potential trauma to the vertebrae and spinal cord in medium-sized dogs. Two screws of 16 mm and 20 mm and rods of 40 mm and 45 mm in length were inserted into the pedicles of L1 and L2 in six dogs. Safe implantation angles for 16 mm screw were 52.67° ± 10.40° and 58.59° ± 7.72° at L1 and L2, respectively. The angle of the 20 mm screw at L1 was recorded at 56.03°±5.34° and 55.67° ± 2.89° at L2. No gross and histological lesion was found on the spinal cord and vertebrae although minimal microfractures of the vertebrae were observed histologically. Findings from this study suggest that CVSRF is feasible for medium-sized dogs using 16 mm screws, however, a long-term study is required to determine the stability and durability of the system.

Keywords: vertebral fracture, luxation, dog, spine

[1]*Department of Veterinary Clinical Studies, Faculty of Veterinary Medicine, Universiti Putra Malaysia, Selangor, Malaysia*
[2]*Department of Clinical Studies, Faculty of Veterinary Medicine, Universiti Malaysia Kelantan, Kelantan, Malaysia*
[3]*Department of Veterinary Pathology and Microbiology, Faculty of Veterinary Medicine, Universiti Putra Malaysia, Selangor, Malaysia*
[4]*Neurology Center, Veterinary Teaching Hospital, Kasetsart University, Bangkok, Thailand*
[5]*Department of Clinical Sciences, Utrecht University, Utrecht, The Netherlands*
****Correspondence**: intannur@upm.edu.my* (N.F. Shafie)
Received July 31, 2022
Accepted September 22, 2022
https://doi.org/10.14456/tjvm.2022.82

Introduction

Vertebral fracture and luxation (VFL) is a devastating condition, accounting for about 7% of all spinal diseases in dogs (Bali *et al*., 2009). The patient may manifest a variety of clinical signs depending on the site of injury and they are usually acute in nature (Jeffery, 2010). The most common site for VFL is the thoracolumbar region and the dog may present with ataxia, paraparesis or paraplegia with or without deep nociception (Bali *et al*., 2009; Jeffery, 2010; Lorenz *et al*., 2011). Surgical treatment is recommended for VFL to improve the chances of recovery, especially with fractures of more than two vertebral compartments that are considered unstable (Shores, 1992; Jeffery, 2010; Hettlich, 2017). Current popular vertebral internal fixation for VFL is a screw or pin with PMMA (Hall *et al*., 2015; Sturges *et al*., 2016; Nel *et al*., 2017). Nonetheless, the major drawbacks of this technique are that it is highly exothermic and radiographically radiopaque with poor osseointegration properties (Ricker *et al*., 2008; Ateş *et al*., 2013; C. Li *et al*., 2020). The temperature for MMA polymerization might vary from 44 °C to 52 °C, which could lead to tissue necrosis. PMMA appears radiopaque in radiograph properties, hence the bone-healing monitoring process will be difficult without advanced diagnostic imaging. Furthermore, the bone-healing process is also affected by poor osseointegration characterized by the adhesion of less osteoblast to the injury site (Gbureck *et al*., 2005; Ricker *et al*., 2008; Robo *et al*., 2018).

The pedicle screw and rod fixation (PSRF) system in humans has been described as a common technique for treating VFL (Michael *et al*., 2016; Wang *et al*., 2017). Its utility in veterinary medicine is extremely limited except in two canine studies (Smolders *et al*., 2012; Özak & Yardimci, 2018), thus the potential of the PSRF system needs to be further explored. Current studies have reported the application of a human PSRF system in the lumbosacral and thoracolumbar region in dogs without complications, although the sizes and dimensions of this human system are not optimal for canine breeds with their large size variation (Özak & Yardimci, 2018). Unfortunately, the PSRF system for adults is too large to be applicable in canine patients even in the largest breeds. The paediatric PSRF system is also very expensive with limited variation in terms of implant sizes, making its application less attractive for dogs. Therefore, the development of a modified PSRF system is required to accommodate the various sizes of canine breeds.

The canine vertebral screw and rod fixation (CVSRF) system is a modified design derived from the PSRF system, which consists of monoaxial side-loaded screw heads. The screw design facilitates the insertion of the screw and titanium rod on the dorsolateral surface of the canine vertebrae, minimizing the risk of trauma to the surrounding tissue (Lewchalermwong *et al*., 2018). To date, the optimal corridors for implantation of this CVSRF have not been determined. A recent study using polyethylene blocks revealed that CVSRF has higher mechanical stiffness compared to screws and PMMA (Lewchalermwong *et al*., 2018). Nevertheless, no data is available on the injury induced by CVSRF on canine vertebrae and spinal cord. The implantation of vertebral screws or rods carries risks of nerve root, spinal cord and vertebral artery injury while the surgical procedure is commonly associated with extensive bleeding and muscle denervation that could potentially lead to ischemia, necrosis and muscle scarring (Dahdaleh *et al*., 2014; Vallefuoco *et al*., 2014; Trindade *et al*., 2016). Implant insertion may also cause microdamage to the bone, leading to implant failure, bone necrosis and bone resorption in severe cases (Abumi *et al*., 2000; Xu *et al*., 2015; Steiner *et al*., 2016). Peri-implant trabeculae microfracture is another common finding that may reduce the mechanical performance of the implant (Steiner *et al*., 2013, 2016; Joffre *et al*., 2017). The objectives of this terminal feasibility study were 1) to determine the safe implantation corridors for the CVSRF system and 2) to investigate its potential trauma to the vertebrae and spinal cord in medium-sized dogs.

Materials and Methods

Animal selection: Ethical application for this terminal animal study was approved by the Institution of Animal Care and Use Committee, Universiti Putra Malaysia (UPM/IACUC/AUP-R022/2018). Six healthy mongrel dogs were received at different times, weighing an average of 17.7 kg (range: 15 to 20 kg) recruited from a local shelter. Physical examination was performed on all dogs at admission and they were found to be fit to undergo general anaesthesia. The dogs were confined in a separate kennel located at the research boarding facility at the University Veterinary Hospital (UVH), UPM. All dogs arrived a day before surgery. Upon arrival, they were bathed and provided with food and water before being fasted for eight hours.

CVSRF system: The CVSRF system used in this study consisted of two screw pairs, 16 and 20 mm with the same diameter of 3.5 mm, two connecting rods with a diameter of 4 mm and a length of 40 mm and 45 mm, and four hexagonal M5 inner screws with thread pitch of 0.8 mm and 4 mm length (Figure 1). All the implant components were manufactured from titanium alloys (Ti 6Al-4V ELI). The implants were applied at the first (L1) and second (L2) lumbar vertebrae. The rod was mounted sideways on the vertebral screw heads. Subsequently, the inner screw was loaded to lock the rod in place.

General anaesthesia and skin preparation: The dogs were induced with tiletamine and zolazepam hydrochloride at 5 mg/kg. They were intubated with an endotracheal tube and maintained with isoflurane using a closed system. The isoflurane level was maintained at 2.5 to 3% with 1 to 1.5% oxygen flow rate. The dogs' vital parameters, such as heart rate, respiration rate, temperature and capillary refill time were monitored every five to ten minutes. Intravenous fluid was also administered at the surgical rate at 5 ml/kg/hr. The surgical area was prepared using a routine skin preparation technique (Tobias & Johnston, 2012). The dorsal area of the twelfth thoracic (T12) to fourth lumbar (L4) was clipped, scrubbed using 4%

diluted chlorhexidine, and dressed with 10% povidone-iodine solution.

Surgical protocol: The implantation of the CVSRF system was achieved via a dorsal approach at the L1 and L2 vertebral bodies. The dog was positioned in sternal recumbency while flexing the thoracic and pelvic limbs. Furthermore, the spine was straightened to achieve a perfect surgical position. A dorsal midline skin incision was made across five vertebrae, T12 to L3, whereas a periosteal elevator was used to retract multifidus musculature laterally away from the dorsal spinous process. The CVSRF system was installed on the left side first using 16 mm screws and 40 mm rod and, subsequently, on the right side using 20 mm screws and 45 mm rod. The insertion of the screws on the left was made at 60°. Additionally, the screws were inserted at the base of the transverse process and caudally to the accessory process. The bone awl was used to mark the screw position, perforating the outer cortex and preparing the passage for the screw. Using the screw inserter, the screws were inserted on L1 before placing the rod sideways on the two screw heads. The inner screws were placed on the head of CVSRF screws to secure the rod in place. Figure 2 shows the final construct for the CVSRF implant. The same procedure was performed on the right side between L1 and L2. A simple continuous pattern was employed to close the muscle, subcutaneous, and skin layers before CT scanning. All surgical procedures were performed by the same surgeon (IS).

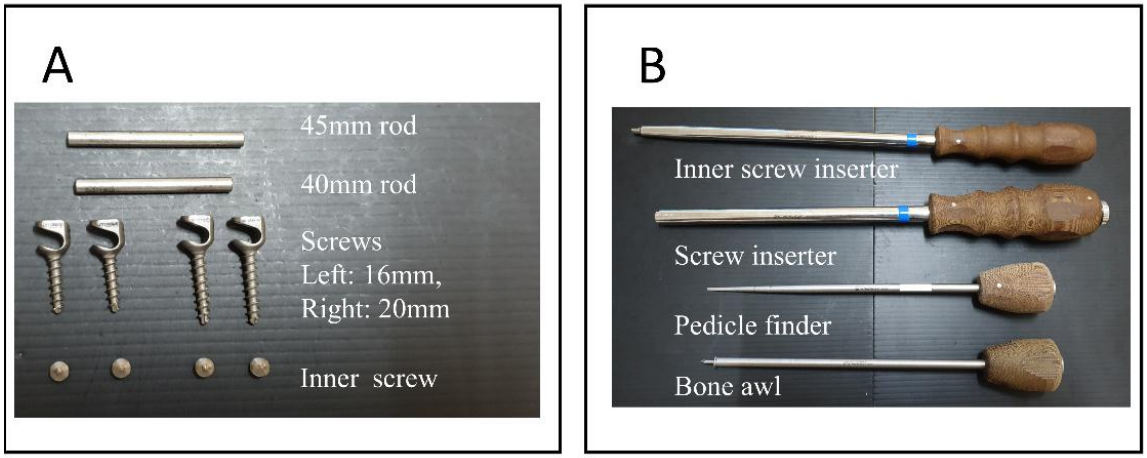

Figure 1 CVSRF system components and instruments. A- Main CVSRF system components which include rod, screws and inner screw. B- Instrument for CVSRF implantation.

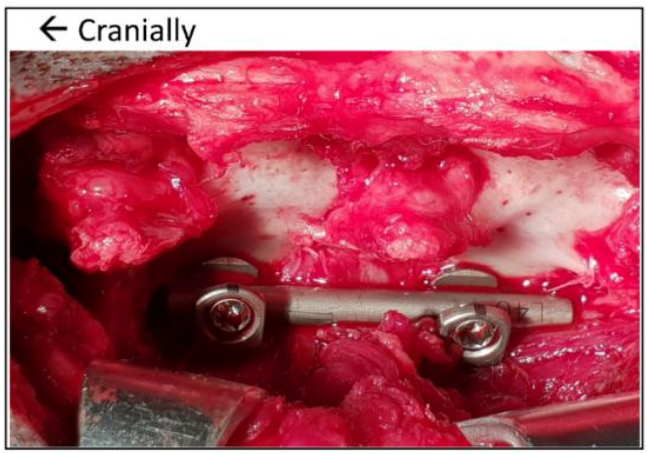

Figure 2 CVSRF system during the surgical procedure in one of the dogs.

Computed tomography (CT) and implantation corridor parameters: Computed tomography (CT) scan was performed with the dogs in dorsal recumbency and the T12 to L4 region was scanned with a cone-beam computed tomography (CBCT) (Fidex; Animage LLC., Pleasanton, CA, USA) using 110kV and 0.15mA. Plain and contrast-enhanced (Iohexol, 800mg/kg, intravenous) CT scans were conducted. After CT, all dogs were overdosed using sodium pentobarbital (Dolethal, Vetoquinol, United Kingdom) at 80 mg/kg without recovering from anaesthesia.

Five parameters were measured in this study; transverse insertion angle of the screw (α), distance of the vertebral body with the aorta (dAo), the distance of the vertebral body with the caudal vena cava (dCvc), the distance of the screw tip with the aorta (dSAo) and the distance of the screw tip with the caudal vena cava (dSCvc). The α of the screw was the angle between the screw and the sagittal plane of the vertebrae. The distance between the vertebral body with the aorta and caudal vena cava was calculated from the most ventral point of the vertebral body to the most dorsal point of

the vessels. The same procedure was repeated to calculate the distance of the screw tip with the aorta and caudal vena cava. All the parameters are illustrated in Figure 3.

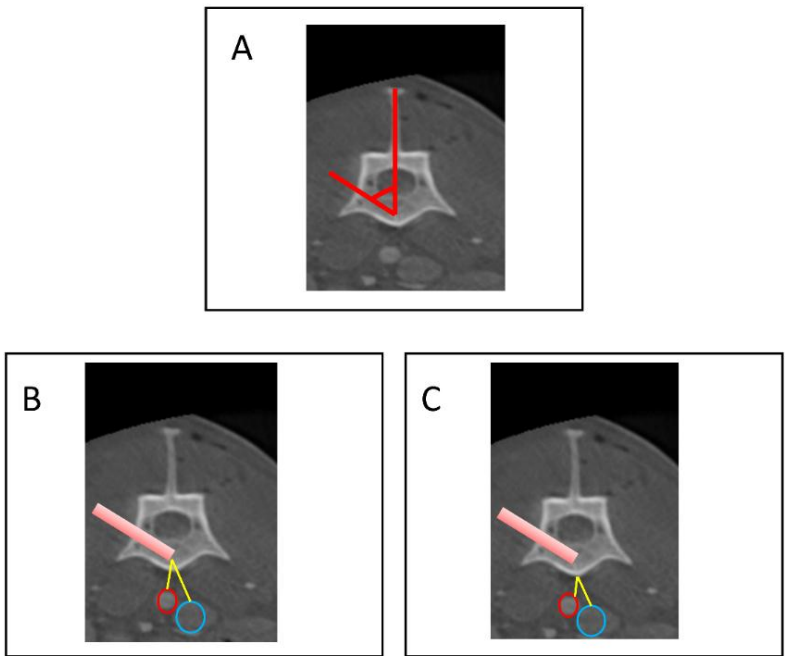

Figure 3 Parameters analysed in CVSRF study. (A) transverse insertion angle of the screw, α. (B) distance of the screw tip with the aorta (red ring), dSAo and distance of the screw tip with the caudal vena cava (blue ring), dSCvc. (C) Distance of the vertebral body with the aorta (red ring), dAo and distance of the vertebral body with the caudal vena cava (blue ring), dCvc.

Post mortem examination of spinal segments: The system was first disassembled from the vertebrae. Then, vertebral segments from T12 to L3 were separated using a bone saw and fixed in 10% neutral buffered formalin (Sigma-Aldrich, USA) for two days. The spinal cord was carefully removed from the spinal canal with forceps. The L1 and L2 spinal cord segments were cut at the point of screw insertion and macroscopically examined for injury and the presence of haemorrhage. Meanwhile, all the surrounding soft tissues were cleaned from the vertebral segments and subsequently decalcified in 10% formic acid (Nacalai Tesque, Japan) solution for up to eight weeks. The L1 and L2 vertebrae were separated from the vertebral segments by severing the intervertebral joint. Then, the vertebrae were cut in the midline and closely examined for macroscopic changes at the pedicle and vertebral body.

***Histological method*:** The tissue samples were dehydrated and paraffinized using a commercial tissue processing machine (Leica TP1020 Semi-enclosed Benchtop Tissue Processor, Leica Biosystem, Germany) for 15 h and 30 mins. The tissues were dehydrated using ethanol gradually at 80% for 2 h, 95% for 2 h, and 100% for 3 h. Thereafter, the tissues were treated with chloroform solution to clear the alcohol for 3 h and lastly with paraffin for wax infiltration for 5 h and 30 mins. The processed tissues were embedded in paraffin blocks (Leica EG1150H and EG11559 Mofular Tissue Embedding Center, Leica Biosystems, Germany). The tissue blocks were sliced in 5 µm thick sections using a microtome (Reichert-Jung 2045 Multicut Rotary Microtome, Leica Biosystems, Germany) and put into the 37 °C water bath before being mounted on glass slides. All the histological slides were stained using Harris' Haematoxylin and Eosin (H&E) and first treated with xylene, 100% alcohol, and 70% alcohol for 5 mins each. After that, the slides were submerged in haematoxylin stain for 5 mins and rinsed with water. The excess colour was removed by using 1% acid alcohol for 3 secs and running water for 5 mins. Then, the slides were stained with Eosin solution for 1 min, and the excess stain was removed using 95% alcohol and subsequently rinsed with running water. A resinous medium was used to dry and preserve the slides. All histology slides were viewed using a microscope (Olympus BX51TF Microscope, Olympus Corporation, Japan).

Parameters: Macroscopically, the vertebrae were examined for frank penetration, lateral and medial encroachment and involvement/perforation of the cortical bone. Histologically, the vertebrae samples were examined for the presence of microfracture and haemorrhage. Samples of the spinal cord were examined for surgical and mechanical injuries, such as indentation, laceration, distraction and shear with the presence of congestion and haemorrhage grossly. Histologically, they were examined for axonal fragmentation, swelling and degeneration, as well as injuries to the arterioles and venules. Evidence of haemorrhage, oedema, infarction and necrosis in the spinal cord was also observed. The spinal cord severity was graded into 0 (normal), 1 (mild), 2 (intermediate), and 3 (severe) as summarized in Table 1.

Data interpretation: All parameters from CT findings were calculated using ImageJ 1.52a (ImageJ software, National Institute of Health, USA). Data was tabulated

in Excel 16.0 (Microsoft Office software, USA) and analysed using Pearson and Shapiro-Wilk for normality test. Given that all the data was normally distributed, the one-way analysis of variance (ANOVA) was applied as the statistical test using GraphPad Prism 7.0 (GraphPad Software, USA). The gross and histopathological findings are presented descriptively.

Table 1 Spinal cord grading and its associate lesions

Grade	Annotations
0 (normal)	No lesion
1 (mild)	Normal neuron with
	Vacuole and granule denaturation of cytoplasm in neurons observed incidentally
2 (intermediate)	Normal neurons and ischemic neurons coexisting in similar numbers,
	Ischemic neurons identified by cytoplasmic eosinophilia with loss of Nissl substance
	And by the presence of pyknotic homogenous nuclei;
	Damage with architectural loss cover 25%-50% of the area
3 (severe)	Many ischemic neurons, crimpled massive neurons, with the nuclear dissolution
	Myelin swelling
	Diffuse damage and architectural loss for more than 50% of the area

Results

Surgical and CT findings: The surgical procedures were performed without major complications in the six dogs. On average, the surgical procedures lasted 2 h and 25 mins of which 25 mins was needed to place the CVSRF system. The transverse view of CT images for both 16mm and 20mm screws are shown in Figure 4. All values for α, dSAo and dSCvc were recorded and no significant difference was observed between the means. The average value for transverse insertion angles of 16 mm screws for L1 and L2 were 52.67° ± 10.40^{o} and 58. 59° ± 7.72^{o}, respectively (Table 2). Meanwhile, the average value for transverse insertion angles of 20 mm screws for L1 and L2 were 56.03° ± 5.34^{o} and 55.67° ± 2.89^{o}, respectively. The closest transverse insertion angle to 60° for 16 mm and 20 mm screws were 59.66° and 59.74°, respectively, whereas the furthest angle to 60° for 16 mm was 40.60° and 48.65° 20 for mm screws.

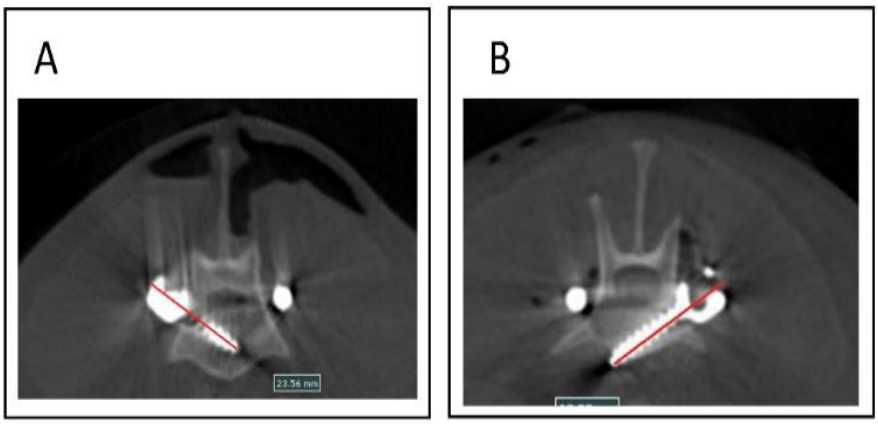

Figure 4 CT images (transverse view) for 16mm screw (A) and 20mm screw (B).

Next, the average distances of 16 mm screw tips to the aorta and caudal vena cava at L1 were 9.21 ± 3.67 mm and 18.96 ± 5.17mm. Contrarily, the average distance for 20 mm screw tips to the aorta and caudal vena cava at L1 were 8.91 ± 2.45 mm and 20.78 ± 6.32 mm (Table 2). At L2, the distances of 16 mm screw tips to the aorta and caudal vena cava were 11.32 ± 1.47 mm and 19.26 ± 5.12mm while that of 20 mm screw tips were 10.23 ± 2.40 mm and 21.15 ± 1.84 mm, respectively. From the 16 mm screws data, the longest distance from the screw tip to aorta was 13.44 mm unlike for 20 mm screws, 12.86 mm. Notably, the shortest distance to the aorta from 16 mm screw tips was 3.94 mm and 5.12 mm for 20 mm screw tips. Lastly, the longest distance from 16 mm and 20 mm screw tips to caudal vena cava were 26.41 mm and 25.77 mm while the shortest were 10.79 mm and 8.25 mm, respectively.

Macroscopic and histopathological findings: Overall, 24 vertebral samples implanted with twelve 16 mm and 20 mm screws each were examined. Frank penetration and lateral or medial encroachment were absent on all of the vertebrae samples when examined grossly. One of the samples (4.2%) had a transverse process fracture on the left side of L1 (16mm screw) during the surgical procedure as the screw was inserted caudally from the landmark. Four (three from 16 mm screws, one from 20 mm screw) of the samples (16.7%) were noticed to be near the vertebral canal (Figure 5B), although no medial encroachment was detected. Twenty-five percent of the vertebral samples were in contiguity with the cortical bone ventrally (Figure 5C) and all were implanted using 20 mm screws. Only 20 out of 24 vertebral samples, 10 each for 16 mm and 20 mm screw, were observed histologically due to sampling processing failure. Histologically, no haemorrhage or tearing of blood vessels was observed in the vertebral tissue samples. Trabeculae

microfractures were only present in the vicinity of insertion for all screws (Figure 6A). There was also evidence of mild cortical damage due to screw penetration as seen in one of the samples microscopically from the 20 mm screw.

The six spinal cord sections examined were normal grossly without any indentation, laceration, distraction, shearing congestion and haemorrhage. Histologically, all six spinal cord samples were graded with grade 1, mild lesion. Since no significant difference was detected in the scoring results, statistical analysis was not performed. Mild cavitation was seen scattered evenly in both the white and grey matter of all spinal cord samples and covering less than 20% of all areas. The nerve cell bodies appeared discoloured but no fragmentations were detected in any of the samples (Figure 7; A&B). The arterioles and venules were found intact and no haemorrhage was observed microscopically but the blood vessels in one of the samples appeared to be congested (16.6%).

Table 2 Mean and standard deviation for implantation corridor parameters for 16mm screws and 20mm screws.

	Mean ± standard deviation	
	16mm screw	**20mm screw**
Lumbar 1		
Transverse insertion angles (º)	52.67° ± 10.40º	56.03° ± 5.34º
Distance between vertebrae and aorta (mm)	6.00 ± 1.14	6.09 ± 1.48
Distance between tip of screw with aorta (mm)	9.21 ± 3.67	8.91 ± 2.45
Distance between vertebrae and caudal vena cava (mm)	15.30 ± 4.07	16.27 ± 5.43
Distance between tip of screw with caudal vena cava (mm)	18.96± 5.17	20.78± 6.32
Lumbar 2		
Transverse insertion angles (º)	58. 59° ± 7.72º	55.67° ± 2.89º
Distance between vertebrae and aorta (mm)	6.82 ± 2.20	6.95 ± 2.30
Distance between tip of screw with aorta (mm)	11.32 ± 1.47	10.23± 2.40
Distance between vertebrae and caudal vena cava (mm)	15.15 ± 2.37	16.58 ± 1.73
Distance between tip of screw with caudal vena cava (mm)	19.26± 5.12	21.15± 1.84

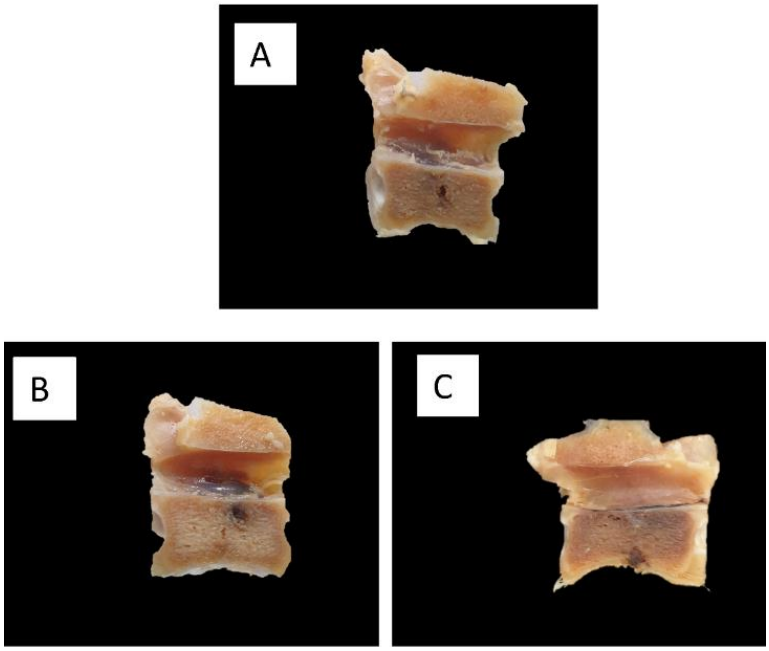

Figure 5 Vertebral section, median plane. **(**A**)** Normal screw penetration on the centre of the vertebral body; **(**B**)** Vertebral canal involvement of screw penetration; **(C)** Cortical involvement of screw penetration.

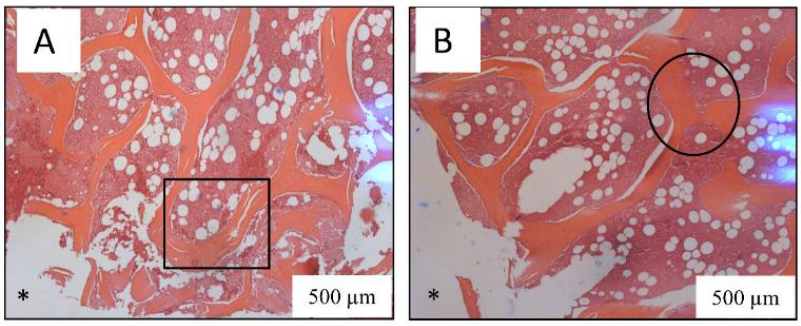

Figure 6 Transverse section through pedicle showing optimal implantation (H&E, 40x). **(A)** Example of a trabeculae microfracture in the vicinity of the implanted screw; **(B)** Example of intact trabeculae *: area of screw penetration; Square: evidence of trabeculae microfracture; Circle: Intact trabeculae.

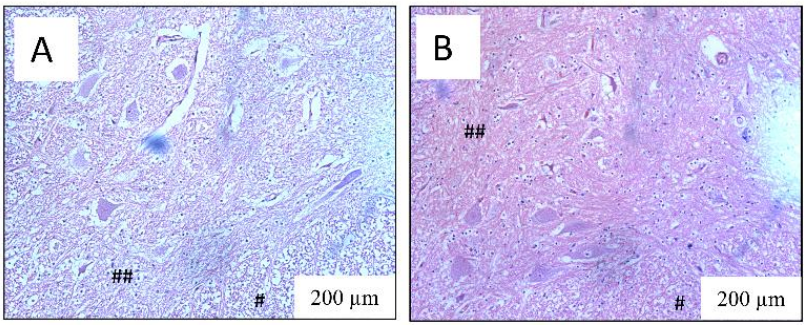

Figure 7 Transverse section of the spinal cord; A-B (H&E, 100x). (A) and (B) - Cavitation of white (#) and grey matter (##). The lesion much more severe in A than in B. The presence of intact neuron cell bodies with discolouration within the grey matter indicates post mortem changes. #: white matter; ##: grey matter.

Discussion

Surgical fixation for VFL is recommended when dealing with unstable fractures (Jeffery, 2010). In this study, the CVSRF system was implanted at a 60° angle in medium-sized dogs at L1 and L2 vertebrae. The recommended guideline suggested insertion between 55° to 65° with 60° as the perfect angle for L1 and L2 (Watine *et al*., 2006). The L1 and L2 vertebrae were chosen as the implantation site as they have wider pedicles than other vertebrae, easily accessible with no rib attachments (Dyce *et al*., 2009). The ventral orientation of the L1 and L2 transverse processes provides ample area for screw insertion and avoids the risk for encroachment. CVSRF was introduced as a solution to the PSRF design problem in dogs. The top-loaded pedicle screw was designed for the dorsal approach (Özak & Yardimci, 2018; Reints Bok *et al*., 2020) thus, is difficult to apply in canine vertebrae with the exception of the lumbosacral region (Smolders *et al*., 2012; Reints Bok *et al*., 2020). In contrast to the pedicle screw, the CVSRF screw possesses a side-loading screw head that allows insertion from lateral to medial which is more feasible for canine patients. The measurement of the total width and height of the vertebrae body through CT and radiographs will assist in selecting the right screw size.

In this study, the range of the insertion angle of the 16 mm screw was between 47° and 67° and between 48° and 64° for the 20 mm screw. Two screws were inserted at an angle less than 47°, i.e., at 40.60° and 42.74°, causing lateral encroachment evidence in CT images but absent in the gross examination of the vertebrae. One fracture that was found at the transverse process of the L1 vertebrae in the gross examination was inserted with a 20 mm screw. The angle of screw insertion was 58°, which was within the recommended guidelines. However, the screw was inserted slightly caudal to the intended landmark. Other than that, neither lateral, medial encroachment nor frank penetration was observed for the screws inserted outside the recommended range both in CT images and gross examination of vertebrae.

These findings indicate that the CVSRF system has a wide safety range of insertion angles, proving that this system is feasible for application in canine patients. Encroachment of the spinal canal was reported in another study when the screws were not in the safe implantation corridor (Smolders *et al*., 2012). The difference in transverse insertion angle between 16 mm and 20 mm screw size was only 0.5°, however, CT revealed that the 20 mm screw exceeded the midline of the vertebral body. Additionally, the distance between the 20 mm screw tip to the aorta and caudal vena cava was 10% less than for the 16 mm screw, which was also observed grossly where six 20 mm screws were close to the cortical bone at the ventral aspect grossly and histologically. CT scan and gross examination both implied that 20 mm screws were too long to be implanted in medium-sized dogs, thus increasing the penetration risk to the aorta and caudal vena cava. Penetration or even laceration to these anatomical structures may cause massive haemorrhage and may affect the dog's survival during the implantation procedure (Tran *et al*., 2017).

Reports on histological findings include examination of the trabeculae microfracture, which commonly occurs post-implantation (Pellegrini *et al*., 2016; Steiner *et al*., 2016). Histologically, trabeculae

microfractures were only found near the screw insertion in this study. This finding is consistent with previous studies where minimal peri-implant microfracture was observed immediately after surgery (Shea *et al*., 2014; Joffre *et al*., 2017; Z. Li *et al*., 2018), although the long-term effect of the implant was unknown in the present study. The minimal trabeculae microfractures in this study imply that the simple self-tapping screw design is not only easy to implant but also evidently causes less trauma to the surrounding bone. Several studies have conducted the histological assessment of microfractures by decalcifying the vertebra together with the implant to avoid induction of microfractures during implant removal (Leucht *et al*., 2007; Z. Li *et al*., 2018). This was not achieved in this study to prevent damage to the only implant set, however, the microfractures observed in all samples were minimal, suggesting implant removal before decalcification has little impact on the vertebrae.

A trauma-induced spinal cord would appear asymmetrical and fragile with the presence of haemorrhage formed as early as five minutes post-trauma (Cemil *et al*., 2016; Sutherland *et al*., 2017). Neuronal necrosis in grey matter together with axonal degeneration in white matter occurred within 30 minutes to an hour, which can be observed histologically (Egawa *et al*., 2017; Spitzbarth *et al*., 2020). The shape of the spinal cords in this study did not appear swollen, indicating no severe cord trauma during CVSRF implantation as none of the screws penetrated the spinal cord. However, a longer observation period is required to assess the degree of injury and development of oedema in the spinal cord, as well as postoperative complications and implant stability (Josephson *et al*., 2001; Onifer *et al*., 2007; Sutherland *et al*., 2017). No tearing of the venous plexus was found in any samples, which is why the haemorrhage was minimal. Furthermore, no neuronal necrosis was observed except for the discoloration of the neuron cell bodies. Consistent cavitation was detected throughout the grey and white matter in all spinal cord specimens and these findings were most likely due to post-mortem changes as all the cell bodies and axons were intact.

This study revealed that the CVSRF system is feasible and applicable to L1 and L2 vertebrae at insertion angles between 46° to 68° without causing any lateral or medial encroachment. Nevertheless, the observations were only restricted to the surgical period and the immediate post-surgical imaging and therefore no long-term post-surgical follow-up was available. Bone healing, bone remodelling, as well as anchorage and durability of the system could not be accessed due to the study design. Overall, the 16 mm screw is suitable for medium-sized dogs between 15 to 20 kg, as demonstrated in this study. In contrast, the 20 mm screw may be suitable for implantation at L5 to L7 in larger-sized dogs, weighing more than 20 kg according to previous data on pedicle length (Watine *et al*., 2006). In-depth knowledge of vertebral anatomy and its surrounding structures combined with presurgical preparation using all available imaging is considered essential for this surgical procedure to be successful.

Acknowledgements

We thank Universiti Malaysia Kelantan, Malaysia for providing a scholarship for the main author for continuing her study in this field.

References

Abumi K, Shono Y, Ito M and Taneichi H 2000. Pedicle Screw Complications. Spine J. 25: 1–8.

Ateş MB, Motro M, Kovan A, Acar YB, Erverdi N and Gülmez T 2013. Does the Bone Cement Affect Miniscrew Stability? Turk J Orthod. 26(3): 119–128.

Bali MS, Lang J, Jaggy A, Spreng D, Doherr MG and Forterre F 2009. Comparative study of vertebral fractures and luxations in dogs and cats. Vet Comp Orthopaed. 22(1): 47–53.

Cemil B, Gokce EC, Kahveci R, Gokce A, Aksoy N, Sargon MF, Erdogan B and Kosem B 2016. Aged garlic extract attenuates neuronal injury in a rat model of spinal cord ischemia/reperfusion injury. J Med Food. 19(6): 601–606.

Dahdaleh NS, Smith ZA and Hitchon PW 2014. Percutaneous pedicle screw fixation for thoracolumbar fractures. Neurosurg Clin N AM. 25(2): 337–346.

Dyce KM, Sack WO and Wensing CJG 2009. Textbook of veterinary anatomy. 4th ed. Elsevier Health Sciences. 407pp.

Egawa N, Lok J, Washida K and Arai K 2017. Mechanisms of Axonal Damage and Repair after Central Nervous System Injury. Transl Stroke Res. 8(1): 14–21.

Gbureck U, Thull R and Barralet JE 2005. Alkali ion substituted calcium phosphate cement formation from mechanically activated reactants. J Mater Sci-Mater M, 16: 423–427.

Hall DA, Snelling SR, Ackland DC, Wu W and Morton JM 2015. Bending Strength and Stiffness of Canine Cadaver Spines After Fixation of a Lumbar Spinal Fracture-Luxation Using a Novel Unilateral Stabilization Technique Compared to Traditional Dorsal Stabilization. Vet Surg. 44(1): 94–102.

Hettlich 2017. Vertebral fracture and luxation repair. In:, Current techniques in canine and feline neurosurgery. 1st ed. A Shores and BA Brisson (eds.) New Jersey: John Wiley & Sons. 209–233.

Jeffery ND 2010. Vertebral fracture and luxation in small animals. Vet Clin N Am- Small. 40(5): 809–828.

Joffre T, Isaksson P, Procter P and Persson C 2017. Trabecular deformations during screw pull-out: a micro-CT study of lapine bone. Biomech Model Mechan. 16(4): 1349–1359.

Josephson A, Greitz D, Klason T, Olson L and Spenger C 2001. A spinal thecal sac constriction model supports the theory that induced pressure gradients in the cord cause edema and cyst formation. Neurosurgery. 48(3): 636–646.

Leucht P, Kim JB, Wazen R, Currey JA, Nanci A, Brunski JB and Helms JA 2007. Effect of mechanical stimuli on skeletal regeneration around implants. Bone. 40(4): 919–930.

Lewchalermwong P, Suwanna N and Meij BP 2018. Canine vertebral screw and rod fixation system: Design and mechanical testing. Vet Comp Orthopaed. 31(2): 95–101.

Li C, Sun J, Shi K, Long J, Li L, Lai Y and Qin L 2020. Preparation and evaluation of osteogenic nano-MgO/PMMA bone cement for bone healing in a rat critical size calvarial defect. J Mater Chem B. *8*(21): 4575–4586.

Li Z, Müller R and Ruffoni D. 2018. Bone remodeling and mechanobiology around implants: Insights from small animal imaging. J Orthopaed Res. *36*(2): 584–593.

Lorenz MD, Coates JR and Kent M 2011. Handbook of Veterinary Neurology. 5th ed. St Louis: SAUNDERS. 94pp.

Michael T, Stefan H, Annabel D, Cornelius M, Hendrik J, Fabian J and Meffert R. 2016. How safe is minimally invasive pedicle screw placement for treatment of thoracolumbar spine fracturs ? Eur Spine J. 26: 1515–1524.

Nel JJ, Kat CJ, Coetzee GL and Van Staden PJ 2017. Biomechanical comparison between pins and polymethylmethacrylate and the SOP locking plate system to stabilize canine lumbosacral fracture-luxation in flexion and extension. Vet Surg. 46(6): 789–796.

Onifer SM, Rabchevsky AG and Scheff SW 2007. Rat Models of Traumatic Spinal Cord Injury to Assess Motor Recovery. ILAR. 48(4): 385–395.

Özak A, and Yardimci C 2018. Treatment of Traumatic Thoracal Instability with Pedicle Screw-Rod Fixation System in a Dog. Kafkas Univ Vet Fak. *24*(4): 627–630.

Pellegrini G, Canullo L and Dellavia C 2016. Histological features of peri-implant bone subjected to overload. Ann Anat. 206: 57–63.

Reints Bok TE, Van Stee L, Willemsen K, Beukers M, Grinwis GCM and Meij BP 2020. Lumbosacral Fusion Using Instrumented Cage Distraction–Fixation in a Dog with Degenerative Lumbosacral Stenosis. Vet Comp Orthopaed Open, *03*(02): e77–e83.

Ricker A, Liu-Snyder P and Webster TJ 2008. The influence of nano MgO and BaSO4particle size additives on properties of PMMA bone cement. Int J Nanomed. *3*(1): 125–132.

Robo C, Hulsart-Billström G, Nilsson M and Persson C 2018. In vivo response to a low-modulus PMMA bone cement in an ovine model. Acta Biomater. 72: 362–370.

Shea TM, Laun J, Gonzalez-Blohm SA, Doulgeris JJ, Lee WE, Aghayev K and Vrionis FD 2014. Designs and techniques that improve the pullout strength of pedicle screws in osteoporotic vertebrae: Current status. Biomed Res Int. https://doi.org/10.1155/2014/748393.

Shores A 1992. Spinal trauma. Pathophysiology and management of traumatic spinal injuries. Vet Clin N Am- Small, 22(4): 859–888.

Smolders LA, Voorhout G, Van de Ven R, Bergknut N, Grinwis GCM, Hazewinkel HAW and Meij BP 2012. Pedicle Screw-Rod Fixation of the Canine Lumbosacral Junction. Vet Surg. 41(6): 720–732.

Spitzbarth I, Moore SA, Stein VM, Levine JM, Olby NJ, Gjessing KM, Davidson RM, Lewis MJ, Jeffery ND, da Costa RC, Nout-Lomas YS, Fenn J, Granger N, Tipold A, Lim JH and Volk H 2020. Current Insights Into the Pathology of Canine Intervertebral Disc Extrusion-Induced Spinal Cord Injury. FronVet Sci. 7: 1–15.

Steiner J, Ferguson SJ and van Lenthe GH 2016. Screw insertion in trabecular bone causes peri-implant bone damage. Med Eng Phys, 38(4): 417–422.

Steiner J, Ferguson S and van Lenthe H 2013. Screw insertion has a negative impact on peri-implant bone quality.[Online] Available: https://lirias.kuleuven.be/1751173?limo=0. Accessed January 2021.

Sturges BK, Kapatkin AS, Garcia TC, Anwer C, Fukuda S, Hitchens PL, Wisner T, Hayashi K and Stover SM 2016. Biomechanical Comparison of Locking Compression Plate versus Positive Profile Pins and Polymethylmethacrylate for Stabilization of the Canine Lumbar Vertebrae. Vet Surg, 45(3): 309–318.

Sutherland TC, Mathews KJ, Mao Y, Nguyen T and Gorrie CA 2017. Differences in the cellular response to acute spinal cord injury between developing and mature rats highlights the potential significance of the inflammatory response. Front Cell Neurosci. 10: 1–18.

Tobias KM and Johnston SA 2012. Veterinary surgery: small animal. 2nd ed. St Louis: Elsevier. 485pp.

Tran JH, Hall DA, Morton JM, Deruddere KJ and Snelling SR 2017. Accuracy and safety of pin placement during lateral versus dorsal stabilization of lumbar spinal fracture-luxation in dogs. Vet Surg. 46(8): 1166–1174.

Trindade R, Albrektsson T, Tengvall P and Wennerberg A 2016. Foreign Body Reaction to Biomaterials: On Mechanisms for Buildup and Breakdown of Osseointegration. Clin Implant Dent R 18(1): 192–203.

Vallefuoco R, Manassero M, Leperlier D, Scotti S, Viateau V and Moissonnier P 2014. Surgical repair of thoraco-lumbar vertebral fracture-luxations in eight cats using screws and polymethylmethacrylate fixation. Vet Comp Orthop Traumatol. 27(4):306–312.

Wang H, Zhou Y, Li C, Liu J and Xiang L 2017. Comparison of Open Versus Percutaneous Pedicle Screw Fixation Using the Sextant System in the Treatment of Traumatic Thoracolumbar Fractures. Clin Spine Surg. 30(3): 239–246.

Watine S, Cabassu JP, Catheland S, Brochier L and Ivanoff S 2006. Computed tomography study of implantation corridors in canine vertebrae. J Small Anim Pract. 47(11): 651–657.

Xu C, Wei Z, Liu N, Sun F, Chen H, Lin T, Zhang B, Tang T and Lu E 2015. The effect of implant shape and screw pitch on microdamage in mandibular bone. Clin Implant Dent R, 17(2): 365–372.